

Parameterization of hyperpolarized ^{13}C -bicarbonate-dissolution dynamic nuclear polarization

David Johannes Scholz¹ · Angela M. Otto¹ · Josef Hintermair¹ · Franz Schilling^{1,3} · Annette Frank³ · Ulrich Köllisch¹ · Martin A. Janich² · Rolf F. Schulte² · Markus Schwaiger³ · Axel Haase¹ · Marion I. Menzel²

Received: 17 September 2014 / Revised: 7 September 2015 / Accepted: 8 September 2015 / Published online: 8 October 2015
© ESMRMB 2015

Abstract

Objective ^{13}C metabolic MRI using hyperpolarized ^{13}C -bicarbonate enables preclinical detection of pH. To improve signal-to-noise ratio, experimental procedures were refined, and the influence of pH, buffer capacity, temperature, and field strength were investigated.

Materials and methods Bicarbonate preparation was investigated. Bicarbonate was prepared and applied in spectroscopy at 1, 3, 14 T using pure dissolution, culture medium, and MCF-7 cell spheroids. Healthy rats were imaged by spectral–spatial spiral acquisition for spatial and temporal bicarbonate distribution, pH mapping, and signal decay analysis.

Results An optimized preparation technique for maximum solubility of 6 mol/L and polarization levels of 19–21 % is presented; T_1 and SNR dependency on field strength, buffer capacity, and pH was investigated. pH mapping in vivo is demonstrated.

Conclusion An optimized bicarbonate preparation and experimental procedure provided improved T_1 and SNR values, allowing in vitro and in vivo applications.

Keywords Hyperpolarized ^{13}C · NMR spectroscopy · MCF-7 · Cell spheroids

Abbreviations

ADC	Apparent diffusion coefficient
BiC	Bicarbonate
CSA	Chemical shift anisotropy
DNP	Dynamic nuclear polarization
EDTA	Ethylenediaminetetraacetic acid
FID	Free induction decay
FOV	Field of view
MRI	Magnetic resonance imaging
PBS	Phosphate buffered saline
TRIS	Tris(hydroxymethyl)-aminomethane

Introduction

Hyperpolarized ^{13}C metabolic MR using ^{13}C -bicarbonate can be used to determine preclinically pH in vivo [1–4]. pH serves as a key parameter in many disorders [5], with cancer being among the most commonly investigated [6–8]. Bicarbonate is a major pH buffer in living systems (blood concentration 25 mmol/L), keeping pH within tight boundaries (pH = 7.35–7.45). Bicarbonate binds with excess protons (decreased pH in vivo) forming carbonic acid. Upon dissociation into water and CO_2 , the latter can be exhaled and the pH returns to physiological values. The reverse occurs when protons are lacking and the pH increases above blood pH. Here, CO_2 and water form carbonic acid, and a proton is released during the conversion of carbonic acid into bicarbonate. In vivo, these reactions are catalyzed by the enzyme family of carbonic anhydrases, with up to 10^6 reactions per second, which leads to a nearly instantaneous pH-dependent equilibrium between bicarbonate and CO_2 concentration. According to Henderson–Hasselbalch, the concentrations of both bicarbonate and CO_2 can be related directly to the pH (see Eq. 1), where pK_a is

✉ Marion I. Menzel
menzel@ge.com

¹ Institute of Medical Engineering, Technische Universität München, Munich, Germany

² Institute of Medical Engineering, General Electric Global Research, Freisinger Landstraße 50, 85748 Garching b. Munich, Germany

³ Nuklearmedizinische Klinik und Poliklinik, Klinikum rechts der Isar, Technische Universität München, Munich, Germany

the dissociation constant and assumed to take on the value of 6.17 *in vivo* [9]:

$$\text{pH} = \text{pKa} + \log_{10} \frac{[\text{HCO}_3^-]}{[\text{CO}_2]} \quad (1)$$

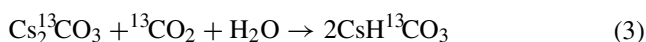
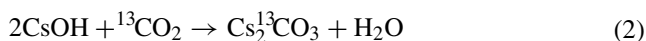
Via dissolution dynamic nuclear polarization (DNP) a signal enhancement of carbon-13 atoms by a factor of >10,000 can be achieved [10]. However, only a few publications provide detail on experimental factors (i.e. buffer capacity, viscosity, pH, magnetic field strength, temperature) that directly affect ^{13}C -bicarbonate and $^{13}\text{CO}_2$ T_1 relaxation times, the achievable signal, and thus pH-mapping quality for *in vitro* or *in vivo* applications. Neglecting these influences may lead to increased signal attenuation in pH-imaging experiments, where $^{13}\text{CO}_2$ needs to be produced from ^{13}C -bicarbonate and subsequently imaged. Since at normal tissue pH, CO_2 concentration and the corresponding signal is at least an order of magnitude smaller than the ^{13}C -bicarbonate signal, $^{13}\text{CO}_2$ imaging is only possible using an experimental setup, where ^{13}C -bicarbonate exhibits maximum SNR and T_1 values. Thus, signal conservation was the primary goal while preparing and performing experiments.

In this work, it is shown that optimizing multiple chemical, biological, and physical parameters at sample preparation and dissolution steps has a large impact on SNR and T_1 decay, illustrating the prohibitive constraints for pH mapping. To achieve sufficient SNR, a formulation for hyperpolarizing ^{13}C -bicarbonate was developed and extensively analyzed in terms of maximizing solubility, radical concentration, gadolinium concentration, and optimizing solid- and liquid-state polarization buildup and decay parameters. The results led to higher concentrations and improved SNR and T_1 for the hyperpolarized compound. Still, the signal origin (intra- or extracellular) of the measured pH, when using hyperpolarized ^{13}C -bicarbonate, is undetermined. It could be separated by their respective apparent diffusion coefficients (ADCs), which are different for intra- and extracellular space [11, 12]. Prior to using this approach, however, SNR and T_1 need to be sufficient for a cell environment. To this end, a dissolved ^{13}C -bicarbonate sample was added to an *in vitro* solution of MCF-7 spheroid cells to investigate its influence on SNR and T_1 in different environments (pure dissolution buffer, culture medium, and highly concentrated MCF-7 cell spheroid solution) for field strengths of 1, 3, and 14 T. Additionally, different pH levels were tested and controlled by electrode pH measurements. Finally, *in vivo* perfusion experiments were performed, showing the time-dependent distribution of the hyperpolarized ^{13}C -bicarbonate in different healthy rat organs (heart, liver, kidney, and bowel).

Materials and methods

Synthesis and preparation of ^{13}C -Cs-bicarbonate for dissolution

^{13}C -sodium bicarbonate was initially tested, but exhibited very limited solubility, thus cesium was chosen (better solubility due to larger counter ion, lower grid enthalpy). For the synthesis, 1.3 g cesium hydroxide monohydrate (Sigma Aldrich, CAS: 35103-79-8) was mixed with 20 mL H_2O to a concentration of 0.389 mol/L and stirred under a $^{13}\text{CO}_2$ (Sigma Aldrich/Euriso-top) atmosphere, monitoring the pH value continuously until a value of ~7 was established, marking the completion of the following reaction:



The ^{13}C -Cs-bicarbonate solution was subsequently lyophilized; approximately 1.3 g ^{13}C -Cs-bicarbonate was obtained.

Solid-state polarization tests revealed glassing performance for every agent at 1.4 K. For the final ^{13}C -Cs-bicarbonate preparation, 1.3 g of an 80/20 %m glycerol/ D_2O mixture was combined with 1.3 g ^{13}C -Cs-bicarbonate powder using an ultrasonic bath and a heat gun at 60 °C, mixed for 2 h for total dissolution, leading to a clear glass when frozen at 1.4 K. The final ^{13}C -Cs-bicarbonate concentration was 6 mol/L. The compound exhibiting the best polarization properties was subsequently analyzed in terms of dissolution parameters, especially T_1 and polarization level, for maximum SNR. Varying concentrations of buffers, including TRIS and PBS based on H_2O and D_2O , were tested at different pH levels for their impact on the pH and T_1 of the final hyperpolarized ^{13}C -Cs-bicarbonate solution.

MCF-7 cell spheroid preparation

The human breast cancer cell line MCF-7 was maintained as a monolayer culture in Dulbecco's modified Eagle's medium, supplemented with 5 % fetal calf serum (culture medium). To obtain three-dimensional aggregates (spheroids), cells were transferred to spinner flasks and were incubated by gently stirring for up to 6 days at 37 °C and 10 % CO_2 . For cell count, spheroids were treated with a hypotonic buffer (20 mM HEPES, 1.0 mM MgCl_2 , 0.5 mM CaCl_2 , pH 7.2) followed by a 5 % benzalkonium chloride solution in glacial acetic acid to obtain a nuclei suspension for electronic counting (Casy, Schärfe, Germany). Immediately before the ^{13}C -NMR measurements, a spheroid suspension containing 50×10^6 cells was centrifuged ($100 \times g$) and resuspended in 1 mL of cell medium.

Polarization level detection and T_1 estimation

Polarization levels were determined directly after dissolution using a Bruker Minispec mq40 NMR analyzer (Bruker Optik, Ettlingen, Germany) with a fourfold-repeated 20° flip-angle excitation (FID). Thermal polarization was determined using 12-fold Carr–Purcell–Meiboom–Gill (CPMG) pulse trains. T_1 times were measured at field strengths of 1, 3, and 14 T. At 1 T the Bruker Minispec with a 10° flip angle excitation and TR of 10 s was used. The 3 T T_1 measurements were performed using a 3 T GE HDx v23 (GE Healthcare, Milwaukee, WI, USA) with a ^{13}C TR solenoid coil (in-house design) with an excitation flip angle of 10° and TR of 1 s. 14 T measurements were performed using a 600 MHz Bruker spectrometer with Avance III console (Bruker BioSpin, Rheinstetten, Germany) with an excitation flip angle of 10° and TR of 1 s.

All experimental data were corrected for the depletion of the hyperpolarized signal during acquisition and quantified with Matlab (MathWorks, Natick, MA, USA). Spectral data at 3 T were quantified using the AMARES algorithm (jMRUI 4.0) [13]. At 14 T, spectral data were apodized with 15 Hz and peaks integrated with MestReNova (mestrelab Research, Santiago de Compostela, Spain). Hyperpolarized ^{13}C -bicarbonate was dissolved and measured in a final concentration of 25 mmol/L. For 1 T measurements, the pure hyperpolarized dissolution was measured. For the 3 and 14 T measurements, the hyperpolarized liquid was added to 1 mL culture medium and 1 mL spheroid suspension, respectively.

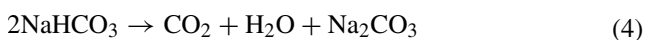
In vivo ^{13}C -bicarbonate imaging

In vivo ^{13}C -bicarbonate imaging was performed on healthy Lewis rats using a custom-designed spectral–spatial excitation pulse (excitation bandwidth 148 Hz, flip angle 10° at ^{13}C -bicarbonate resonance frequency) and spiral trajectory (resolution 16×16 , FOV = 8 cm, slice thickness = 10 mm, TR = 2 s). Five milliliters per kilogram rat weight of a 200 mmol/L ^{13}C -bicarbonate solution was injected through the tail vein and data acquisition started immediately.

Results

Optimizing the hyperpolarization formulation

Although the maximum solubility of bicarbonate in glycerol increases with temperature, for bicarbonate, increasing temperature leads to an increased conversion to carbonate as follows:



This results in very low polarization levels ($\leq 5\%$) for preparation at temperatures $\geq 80^\circ\text{C}$, owing to the loss of bicarbonate; too low temperatures prevent dissolution due to the high viscosity of glycerol. The optimum temperature was determined to be 60°C ; an increased D_2O /glycerol ratio led to a decreased viscosity (allowing lower temperatures). Decreasing the amount of glycerol from 80 to 50 % led to decreased liquid-state polarization from 19–21 to 10–11 %, owing to the better glassing properties of glycerol.

Different OXO63 radical concentrations (14–69 mmol/L) were investigated, with the radical primarily affecting the T_1 relaxation time (increases relaxivity by 0.01 mmol/L/s). The hyperpolarized solid state signal showed limited maximum values for a concentration of ≥ 42 mmol/L. At 14 mmol/L, the solid-state buildup was not yet complete ($< 95\%$) after 2 h of polarization. The liquid-state signal collapsed with OXO at ≥ 42 mmol/L. The optimal radical concentration was found to be approximately 25 mmol/L, which exhibited a desirable solid-state level, an acceptable buildup time (90 min) for $> 99\%$ solid-state polarization, and a desirable liquid-state signal after dissolution. All polarization experiments were performed with an OXO concentration of 25 mmol/L.

Different gadolinium concentrations (ranging from 0 to 3.5 mmol/L) were tested in relation to T_1 (see Fig. 1a), measured at 1 T. Gd increases the maximum achievable solid-state signal, mainly because increasing its concentration leads to higher polarization levels. Gd decreases the T_1 of the electrons involved in the polarization process, thus at 100 mW irradiation (power-saturated regime) the polarization becomes more efficient [14]. Higher Gd concentrations also affected CPMG acquisitions, increasing the error of the estimated polarization. Moreover, T_1 decreases with increasing Gd concentration [15]. An optimal Gd concentration was thus found at 0.5 mmol/L, (tradeoff between increased polarization level and reduced T_1 relaxation time).

Optimal polarization results were achieved for 25 mmol/L radical (OXO) and 0.5 mmol/L Gd (Dotarem). A 200 μL volume of the sample was then polarized for 90 min in a HyperSense DNP polarizer (Oxford Instruments, Abingdon, UK). The hyperpolarized sample was subsequently dissolved with a heated dissolution agent (PBS) with EDTA added (0.1 g/L) at 168°C . The final dissolved solution had a physiological pH, osmolality, and temperature. The pH was controlled externally by a pH electrode. The final polarization level was approximately 19 %.

Optimizing dissolution parameters

To increase T_1 , a D_2O -based, pH-buffered dissolution agent was chosen for in vivo experiments, keeping the pH and osmolality at physiological levels. The bicarbonate itself

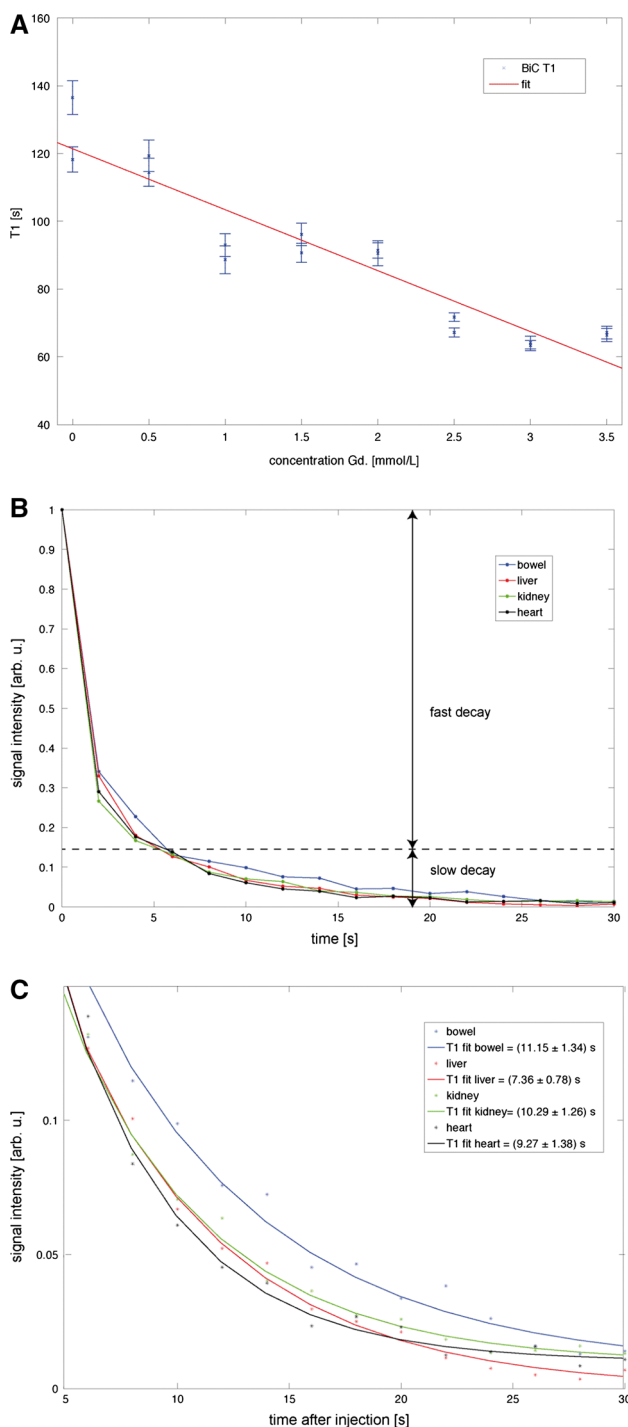


Fig. 1 a Influence of Gd concentration (*horizontal axis*) on T_1 of ^{13}C -Cs-bicarbonate decay after dissolution in D_2O (*vertical axis*). *Error bars* indicate 95 % confidence boundaries of the mono-exponential fit. T_1 decreases with increasing Gd concentration. Two dissolution experiments were performed for each Gd concentration to ensure reproducibility; **b** intravascular ^{13}C -bicarbonate signal intensities for different in vivo cross sections. The *vertical axis* shows the signal intensities, normalized to the highest intensity at $t = 0$ s. The *horizontal axis* shows time after injection in seconds. After 6 s, 85 % of the hyperpolarized signal is decayed (*dotted line*), comparable to a T_1 of approximately 1 s. In this region, parts of the injection bolus pass and the intravascular signal diffuses into extravascular and intracellular regions. The remaining 15 % signal decays with a T_1 of 10 s, which is the part that may be used for pH detection; **c** in vivo T_1 -decay of ^{13}C -bicarbonate, measured for different organ cross sections in a healthy rat. *Error* was calculated using 95 % confidence boundaries of the mono-exponential fit

$$\text{pH} = \text{pH}_{\text{start}} - 0.0028 \times \Delta\text{temp} \quad (5)$$

For simulation, $\text{pH}_{\text{start}} = 7.0$ is assumed. Signal loss was calculated by transforming Eq. (1) to

$$\text{sig}_{\text{loss}} = \frac{100}{\text{sig}_{\text{CO}_2} + 10^{\text{pH}-\text{pKa}}} \quad (6)$$

with $10^{\text{pH}-\text{pKa}} = \text{sig}_{\text{BIC}} = 10$ signal of ^{13}C – bicarbonate; $\text{sig}_{\text{CO}_2} = 1 = \text{signal of } ^{13}\text{CO}_2$; $\text{sig}_{\text{loss}} = \text{percentage of } ^{13}\text{CO}_2$ contributing to the overall signal; and $\text{pKa} = 6.2$, as reported in vivo [2, 9]. When the pH decreases, increasing the temperature during the dissolution process from room temperature to 168 °C leads to a decrease in pH. Hence, the contribution of $^{13}\text{CO}_2$ to the overall signal becomes larger. Assuming that all $^{13}\text{CO}_2$ buildup due to the pH decrease is removed, the signal loss increases from 13.7 % at room temperature to 32.4 % at dissolution temperature. This loss is treated as a full removal of $^{13}\text{CO}_2$ after equilibrium is established. This assumption is simplified owing to the fact that the buildup of the equilibrium is a permanent and dynamic process. In addition, the release of CO_2 is dynamic and, moreover, the dynamics change during the dissolution process. Regardless of the assumptions made, there is a significant impact from the temperature of the dissolution agent, which was taken into account during its preparation.

In vitro application with MCF-7 tumor spheroids

T_1 (at 1, 3 and 14 T) and SNR of the hyperpolarized ^{13}C -bicarbonate signal of the culture medium with and without MCF-7 tumor spheroids were investigated (see Table 1) using 10° excitation and subsequent FID readout. The pH values were controlled by a common glass electrode. At 1 T, the T_1 of ^{13}C -bicarbonate, dissolved in a D_2O -based phosphate buffer, showed a decrease with decreasing pH or increased phosphate concentration. At 3 T, the T_1 of ^{13}C -bicarbonate and $^{13}\text{CO}_2$ were measured with and without added MCF-7 cell spheroids. $^{13}\text{CO}_2$ showed similar

acts as a pH buffer, though the pure Cs-bicarbonate dissolution showed pH values of 8.2–8.4, so the final pH needed to be balanced with the dissolution agent buffer to preserve ^{13}C -bicarbonate (at lower pH $^{13}\text{CO}_2$ gets released during the turbulent dissolution process). Furthermore, depending on the buffer used, the temperature of the dissolution liquid (heated to 168 °C during dissolution) might affect the pKa and thus the pH. The pH change of the phosphate buffer [16] was thus described as:

Table 1 T_1 times and errors for ^{13}C -bicarbonate and $^{13}\text{CO}_2$ in culture medium (orange), cell spheroid suspension (green), and pure dissolution (blue) for 1, 3, and 14 T

	exp1	exp2	exp3	exp4	exp5	exp6	exp7
ph_DA	7.11	7.11	7.11	7.32	6.26	5.17	5.13
c_DA [mmol/L]	40	40	40	40	40	40	120

		T_1 [s]													
		$T_1 \pm \text{err}$		$T_1 \pm \text{err}$		$T_1 \pm \text{err}$		$T_1 \pm \text{err}$		$T_1 \pm \text{err}$		$T_1 \pm \text{err}$		$T_1 \pm \text{err}$	
1 T															
BiC decay		83.27	1.01	93.41	1.4	91.85	0.93	93.98	1.54	85.68	1.63	79.69	0.93	76.05	1.37
3 T															
BiC decay		54.08	0.23	53.97	0.09	56.92	0.16	60.24	0.22	61.92	0.12	56.31	0.09	42.53	0.09
CO ₂ decay		55.16	0.81	55.16	0.81	53.88	1.33	53.34	0.64	58.24	0.44	54.56	0.41	41.79	0.19
CO ₂ buildup		9.39	0.76	10.46	1.07	12.31	1.83	9.88	0.63	8.65	0.92	9.29	0.76		
14 T															
BiC decay		43.16	0.63	42.01	0.65	43.65	0.63	37.25	0.21	37.62	0.22	38.15	0.28	38.01	0.58
CO ₂ decay		41.24	5.78	57.3	6.09	57.17	7.99	40.63	4.59	49.65	3.35	52.61	4.26	25.01	2.95

Yellow boxes show the pH and the concentration of the phosphate buffer used to dissolve the hyperpolarized ^{13}C -bicarbonate. The T_1 of ^{13}C -bicarbonate and $^{13}\text{CO}_2$ decrease with increasing field strengths. Also, decreasing the pH and increasing the buffer concentration leads to a decrease in T_1 . All decays show a mono-exponential behavior, except for the 3 T CO₂ signal, where the experimental setup allowed a more rapid tracking of CO₂ buildup. The observed CO₂ buildup points to an insufficient presence and activity of carbonic anhydrases in the solutions, which prevents an instantaneous establishment of the equilibrium. Bi-exponential fitting allows for the extraction of a CO₂ buildup constant, which was similar for all experiments performed. Error was calculated using 95 % confidence boundaries of the fit

T_1 values, compared to ^{13}C -bicarbonate for measurements with added MCF-7 cell spheroids. The T_1 of ^{13}C -bicarbonate was only increased in the culture medium; it decreased when cells were added to the solution. This T_1 decrease was not detectable for $^{13}\text{CO}_2$ where T_1 did not decrease significantly following spheroid addition. The bicarbonate's T_1 is decreased by fast exchange with multiple weak binding sites of macromolecules in the suspension. After the T_1 experiments, the pH of the spheroid suspension was controlled with a pH electrode and showed a decreasing pH with time. This is an indication of ongoing cell metabolism. During this time, the highly concentrated cell solution acidifies its environment. The measurements at highest buffer concentration and lowest pH (far right column, Table 1) showed a significant drop in T_1 for both bicarbonate and CO₂, and no CO₂ buildup was observed. These results show the clear influence of field strength on bicarbonate T_1 , as well as the sample's viscosity on the physical side. On the chemical side, increasing pH and buffer capacity leads to a decreased T_1 .

In vivo imaging on healthy Lewis rats

The hyperpolarized ^{13}C -bicarbonate solution was injected via a tail vein, and data acquisition began immediately

after injection. The bicarbonate kinetics were acquired with $\Delta t = 4$ s for four cross sections: heart, liver, kidney, and bowel (see Fig. 2).

The heart cross section, measured directly after injection ($t = 0$ s), showed a distribution of ^{13}C -bicarbonate only in the right ventricle, as expected, where it arrived after injection and spread to the left ventricle with increasing time. Liver, kidney, and bowel sections showed ^{13}C -bicarbonate concentration predominantly in the vena cava. The liver sections only showed ^{13}C -bicarbonate in the vena cava. Although the liver is well perfused, no bicarbonate signal became visible in the surrounding tissue. This might be owing to the presence of paramagnetic centers to which the bicarbonate can bind, which reduces T_1 . The kidney section showed maximal ^{13}C -bicarbonate concentration directly after injection. This reflects the high perfusion of the kidneys. Bowel tissue is well perfused at $t = 0$ s and the signal decays with increasing time. The decay of the ^{13}C -bicarbonate signal can be attributed to multiple factors; the hyperpolarized signal completely decays in vivo with a T_1 of approximately 10 s. In addition, the hyperpolarized signal is consumed for every excitation. Meanwhile, the bicarbonate is filtered by the kidneys, converted by the liver, constantly converted to CO₂ in the blood and tissue, and subsequently exhaled.

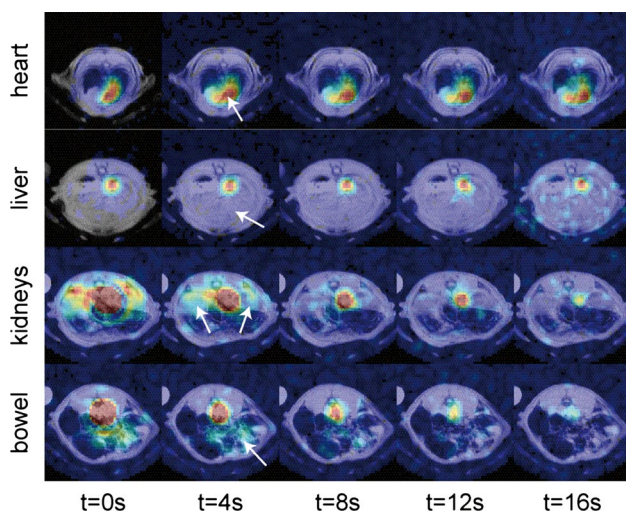
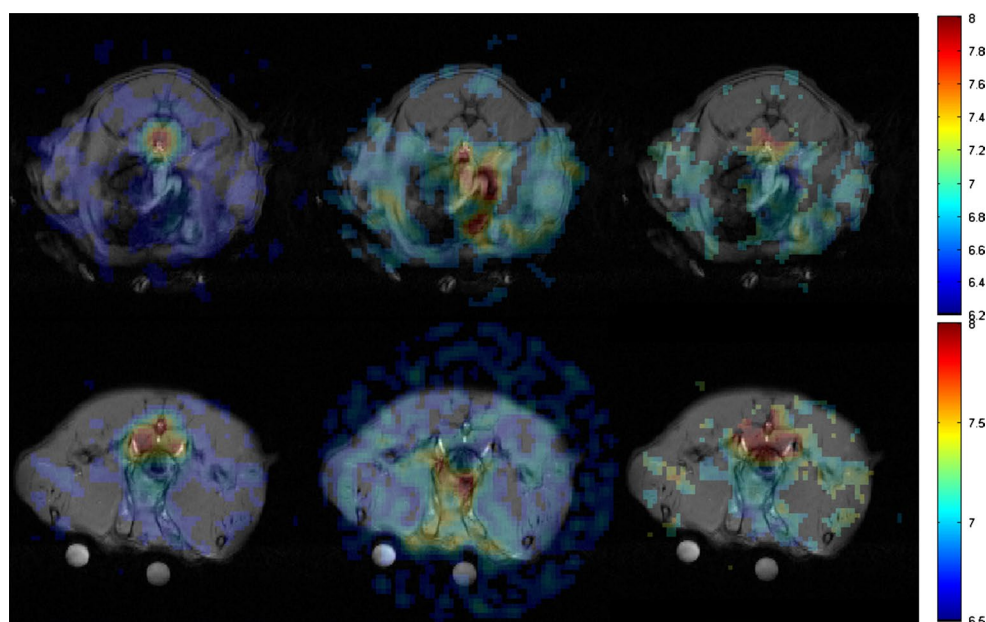


Fig. 2 ^{13}C -bicarbonate signal after a tail-vein injection (21 s after dissolution) of approximately 1 mL hyperpolarized solution at different times for different cross sections. Positions of organs are marked with white arrows in the $t = 4$ s series. A 10° FA excitation was used, with frequency selective spectral spatial pulses, applied on resonant at the ^{13}C -bicarbonate resonance frequency, and subsequent spiral trajectory readout. Cross section thickness = 10 mm, FOV = 8 cm \times 8 cm. Signals from the heart and liver were normalized to maximum peak intensity. Signals for kidney and bowel were normalized to a fixed value for better visibility of bicarbonate in the peripheral tissue

In vivo bicarbonate, CO_2 and the resulting pH map for exemplary cross sections through the bowel and hind legs of a healthy rat are depicted in Fig. 3. The pH is only calculated in image areas, where both bicarbonate and CO_2 images exhibit signal intensity about the mean noise level, i.e. in the bowel region, the central area around the blood vessel.

Fig. 3 In vivo (from left to right) ^{13}C -bicarbonate, $^{13}\text{CO}_2$, and pH images of a healthy Lewis rat, depicting bowel (top row) and leg region. pH was calculated in ROI above the mean noise level only, exhibiting strong signals in the central area around the blood vessel and the intestines



Determination of ^{13}C -bicarbonate T_1 in vivo

The longitudinal signal evolution of the hyperpolarized ^{13}C -bicarbonate was investigated with the aim of identifying a suitable time to begin image acquisition. Determination of this T_1 decay was performed by using a voxel of highest intensity at $t = 0$ s within the acquired intensity map (see Fig. 2), which was found to be mainly intravascular because of the bolus. After ^{13}C -bicarbonate injection via the tail vein, a rapid decay of the hyperpolarized signal of ^{13}C -bicarbonate could be observed within 6 s (see Fig. 1b). This initial, rapid decay is dominated by the fading of the bolus signal and most likely due to perfusion into smaller blood vessels. Additional contributions to signal decay are due to the diffusion and transport in the peripheral tissue, kidney filtration, and CO_2 conversion and exhalation. From this data, ^{13}C -bicarbonate perfusion equilibrated at around 6 s, reaching a steady state, after which in vivo pH measurements could be performed. After the injection bolus has passed, the signal decayed with a T_1 of around 10 s for all cross sections (see Fig. 1c). These values are comparable with in vivo values previously published [2].

Discussion

In this work, the process of hyperpolarization of ^{13}C -bicarbonate was investigated quantitatively, in terms of preparation and dissolution parameters. Because of the sensitivity of ^{13}C -bicarbonate to temperature and pH, these parameters must be controlled carefully during experiments to achieve a sufficiently high concentration and T_1 for a maximum SNR. T_1 analysis for the hyperpolarized

compound showed sufficiently long decay times for all investigated field strengths, and the effects of pH, buffer capacity, and viscosity on ^{13}C -bicarbonate T_1 were analyzed. A lowered pH led to a reduced T_1 , which should be taken into account when investigating conditions with symptomatically low pH, as in cases of tumor acidification or inflammatory diseases. In addition, low pH inhibits the enzymatic activity of carbonic anhydrase, leading to a slower establishment of the pH-dependent bicarbonate to CO_2 ratio at more acidic pH values. It was shown that the T_1 and SNR were high enough to prompt further investigations, even at higher field strengths, i.e., applying the diffusion-based approach for intra and extracellular signal determination measured with MCF-7 cell spheroids, which has been shown to work at 14 T with MCF-7 cell spheroids [11] and 4.7 T in animals [12] for hyperpolarized [$1\text{-}^{13}\text{C}$]pyruvate, and may be successfully applied to ^{13}C -bicarbonate. This allows the determination of the signal contribution of intracellular signals, and hence the impact on hyperpolarized ^{13}C -bicarbonate pH measurements. Moreover, the intravascular in vivo T_1 values of ^{13}C -bicarbonate are sufficiently long in different organs, and are comparable to previously published values [2]. However, the distribution of bicarbonate is dependent on the target organ, which makes it difficult to estimate an ideal measurement time frame and needs to be investigated in each case. In general, bolus detection should be avoided to minimize errors, which arise from the variation in perfusion between organs. Because of the very low $^{13}\text{CO}_2$ signal intensity, multiple excitations and acquisition of $^{13}\text{CO}_2$ kinetics were not feasible. Therefore, imaging is limited to acquisition schemes using configurations such as a 90° flip-angle excitation for $^{13}\text{CO}_2$. To determine spatial pH, a high SNR of both the ^{13}C -bicarbonate and $^{13}\text{CO}_2$ signals is needed. Hence, it is crucial to determine the ideal time point of acquisition, where the hyperpolarized ^{13}C -bicarbonate is diffused to the targeted tissue and the signal has not decayed. Most of the ^{13}C -bicarbonate signal is lost within the first few seconds as the bolus is passed, leading to a residual signal of only 15 %. The remaining signal can be assumed to be non-perfusion-dominated, leading to T_1 times of around 10 s, which are comparable with values reported previously [2]. To lose such a high amount of signal within the first seconds raises the question of whether a systemic injection through the tail vein might not be optimal for pH mapping, since breathing and kidney filtration effectively removes the hyperpolarization-labeled substances. Thus, injection could be performed in a vein or artery closer to the targeted organ, which should reduce the initial signal loss. Hence, more time would be allotted for diffusion through the tissues and the buildup of the $^{13}\text{CO}_2$ pool required for acquisition.

Conclusion

The preservation of hyperpolarized signals is crucial for the application of hyperpolarized ^{13}C -bicarbonate in dissolution-DNP experiments. SNR is heavily dependent on parameters involved in both sample preparation and experimental procedure. Carefully tuning these parameters helps avoid pitfalls in signal depletion, resulting in sufficient, though not excellent, SNR and T_1 for in vivo ^{13}C -bicarbonate and pH mapping.

Acknowledgments D.J.S. gratefully acknowledges Sean Bowen for helpful discussions. Also, he acknowledges the support of the Graduate School of Information Science in Health at Technische Universität München. This work was supported by a grant from the German Bundesministerium für Bildung und Forschung (BMBF, FKZ 13EZ1114). The authors take responsibility for the content of the publication. The research leading to these results received funding from the European Union Seventh Framework Program (FP7) under Grant Agreement No. 294582 ERC Grant MUMI.

Compliance with ethical standards

Conflict of interest D.J.S.: material support from GE Global Research; M.I.M, R.F.S, M.A.J.: employment at GE Global Research.

Ethical standard All animal studies have been approved by the local governmental committee for animal protection and welfare (Tierschutzbehörde, Regierung von Oberbayern) and have therefore been performed in accordance with the ethical standards laid down in the 1964 Declaration of Helsinki and its later amendments. The manuscript does not contain clinical studies or patient data.

References

1. Lau AZ, Chen AP, Ghugre NR, Ramanan V, Lam WW, Connelly KA, Wright GA, Cunningham CH (2010) Rapid multislice imaging of hyperpolarized ^{13}C pyruvate and bicarbonate in the heart. *Magn Reson Med* 64(5):1323–1331
2. Gallagher FA, Kettunen MI, Day SE, Hu D-E, Ardenkjaer-Larsen JH, Rit Zandt, Jensen PR, Karlsson M, Golman K, Lerche MH, Brindle KM (2008) Magnetic resonance imaging of pH in vivo using hyperpolarized ^{13}C -labelled bicarbonate. *Nature* 453(7197):940–943
3. Schroeder MA, Swietach P, Atherton HJ, Gallagher FA, Lee P, Radda GK, Clarke K, Tyler DJ (2010) Measuring intracellular pH in the heart using hyperpolarized carbon dioxide and bicarbonate: a ^{13}C and ^{31}P magnetic resonance spectroscopy study. *Cardiovasc Res* 86(1):82–91
4. Scholz DJ, Janich MA, Köllisch U, Schulte RF, Ardenkjaer-Larsen JH, Frank A, Haase A, Schwaiger M, Menzel MI (2015) Quantified pH imaging with hyperpolarized ^{13}C -bicarbonate. *Magn Reson Med* 73(6):2274–2282
5. Adrogue HJ, Madias NE (1998) Management of life-threatening acid–base disorders. *N Engl J Med* 338(1):26–34
6. Warburg O (1956) On the origin of cancer cells. *Science* 123(3191):309–314
7. Vaupel P, Kallinowski F, Okunieff P (1989) Blood flow, oxygen and nutrient supply, and metabolic microenvironment of human tumors: a review. *Cancer Res* 49(23):6449–6465

8. Zhang X, Lin Y, Gillies RJ (2010) Tumor pH and its measurement. *J Nucl Med* 51(8):1167–1170
9. Deane N, Smith HW (1957) The apparent first dissociation constant, pK_1' , of carbonic acid in the human erythrocyte. *J Biol Chem* 227(1):101–106
10. Ardenkjaer-Larsen JH, Fridlund B, Gram A, Hansson G, Hansson L, Lerche MH, Servin R, Thaning M, Golman K (2003) Increase in signal-to-noise ratio of >10,000 times in liquid-state nmr. *Proc Natl Acad Sci USA* 100(18):10158–10163
11. Schilling F, Duwel S, Kollisch U, Durst M, Schulte RF, Glaser SJ, Haase A, Otto AM, Menzel MI (2013) Diffusion of hyperpolarized (13 C)-metabolites in tumor cell spheroids using real-time nmr spectroscopy. *NMR Biomed* 26(5):557–568
12. Sogaard LV, Schilling F, Janich MA, Menzel MI, Ardenkjaer-Larsen JH (2014) In vivo measurement of apparent diffusion coefficients of hyperpolarized (13 C)-labeled metabolites. *NMR Biomed* 27(5):561–569
13. Naressi A, Couturier C, Castang I, De Beer R, Graveron-Demilly D (2001) Java-based graphical user interface for mrui, a software package for quantitation of in vivo/medical magnetic resonance spectroscopy signals. *Comput Biol Med* 31(4):269–286
14. Lumata L, Kovacs Z, Sherry AD, Malloy C, Hill S, van Tol J, Yu L, Song L, Merritt ME (2013) Electron spin resonance studies of trityl ox063 at optimal concentration for DNP. *Phys Chem Chem Phys* 15(24):9800–9807
15. Ardenkjaer-Larsen JH, Macholl S, Jóhannesson H (2008) Dynamic nuclear polarization with trityls at 1.2 k. *Appl Magn Reson* 34(3–4):509–522
16. Ellis KJ, Morrison JF (1981) Buffers of constant ionic strength for studying pH-dependent processes. *Method Enzymol* 87:405–426